



ACOUSTICS 2012

SPPS, a particle-tracing numerical code for indoor and outdoor sound propagation prediction

J. Picaut and N. Fortin

Département Infrastructures et Mobilité (IFSTTAR/IM), Route de Bouaye, CS4, 44344
Bouguenais Cedex
judicael.picaut@ifsttar.fr

Geometrical and energetically models are widely used in outdoor and indoor noise predictions. Several approaches have been considered, amongst them, one can cited the ray and beam-tracing methods, the image-source method, the radiosity method, etc. Another approach is based on the use of sound particles to model the sound propagation in complex environments. Similarly to the ray-tracing methods, the sound particles concept allows to model many acoustics phenomena like absorption, transmission, réflexion and diffusion on surfaces, scattering by fitting objects, meteorological effects, etc. Two approaches can be followed: a probabilistic one, considering that the energy that is carried by the particle is constant and using Monte-Carlo methods for the modelling of acoustics phenomena; a deterministic one, considering that the energy of sound particles is modified according to the acoustics phenomena. In this paper, a numerical code (SPPS), using both approaches is presented and many applications are shown. In addition, several comparisons with experimental data and other methods are also proposed.

1 Introduction

Sound field modelling in architectural acoustics lies at the origin of a large number of studies within the scope of room and environmental acoustics. The objective is to propose models for accurate prediction of sound fields, some of them in order to virtually simulate room acoustics using auralization techniques [1]. Given the complexity of the task, several approaches have been considered, from which on can cited energetic approaches, like the classical reverberation theory or the image-sources, ray-tracing [2] and radiosity methods [3], etc. More recently, undulatory approaches like the finite-difference time-domain [4] and the transmission line matrix [5] methods have also been proposed. However, they are still limited due to significant computational times. Thus, energetic approaches are still relevant today. Particularly, the particle-tracing method is an interesting alternative approach, quite similar to the ray-tracing method, which is able to consider the main physical phenomena involved during sound propagation.

Although the sound particles concept was first introduced by Joyce [6], the first practical implementation for room acoustics was conducted by Stephenson [7], who showed the tremendous potential of the method for modeling complex propagation phenomena..

Following the same approach, the sound particles concept was fully implemented in a numerical code for three-dimensional (3D) complex environments. A special attention was paid to consider all major physical phenomena occurring during sound propagation, and to optimize algorithms in order to reduce computational times.

2 Presentation of the method

2.1 Principle

The simulation principle relies upon tracking sound particles, carrying a amount of energy ε and emitted from a sound source, within a 3D-domain [8]. Each particle propagates along a straight line between two time steps Δt (the whole trajectory may be curved), until collision with an object. At each collision, sound particles may be absorbed, reflected, scattered, diffused, transmitted, depending on the nature of the object.

Two algorithms can be considered. The first approach is to consider that the energy of the particle is constant. In function of the phenomena, the particle may disappear from the domain or follows its propagation: the number of sound particles decreases along the time. In the second approach, the particle energy is varying according to the

physical phenomena occurring during the propagation. In this case, the number of particles in the domain should be constant along the time. Since, in both cases, physical phenomena can be modeled according to probabilistic laws, both approaches are equivalent to Monte-Carlo methods. The accuracy of prediction is then dependent of the initial number of particles.

2.2 Algorithms

2.2.1 Sound source modelling

2.2.1.1 Directivity Sound emission from a point source can be modeled by considering that sound particles, at the emission time and at the exact position of the source, propagate in directions in accordance with the source directivity. It is then necessary to verify that the number of particles emitted by elementary solid angle $d\Omega = d\phi \sin \theta d\theta$ is in accordance with the directivity of the source $Q(\theta, \phi)$.

For example, in the case of an omnidirectional sound source, sound particles have to be uniformly distributed over a sphere centered on the source, meaning that angle (θ, ϕ) must be chosen according to the following relations:

$$\phi = 2\pi \times u \in [0, 2\pi], \quad (1)$$

$$\theta = \cos^{-1}(2v - 1) \in [0, \pi]. \quad (2)$$

where u and v are two random numbers between 0 and 1 (uniform distribution). The same approach can also be applied to non-uniform directivity. At the present time, only omni- and mono-directional point sources, and planar sources are modeled in the SPPS code.

2.2.1.2 Initial sound particle energy During a time step Δt , a source with a sound power W emits an amount of energy $E = W \times \Delta t$. In the sound particle concept, each particle carries an initial energy ε_0 . If the source emits N sound particles, the energy conservation between both approaches requires:

$$N \times \varepsilon_0 = W \times \Delta t, \quad (3)$$

meaning that the initial energy of a sound particle is given by

$$\varepsilon_0 = \frac{W}{N} \times \Delta t. \quad (4)$$

2.2.2 Propagation modelling

2.2.2.1 Free field propagation In free field condition and without absorption, the theoretical decrease of sound intensity from a point source, in the direction (θ, ϕ) , is:

$$I(\theta, \phi) = \frac{Q(\theta, \phi)}{4\pi r^2}, \quad (5)$$

where r is the distance from the source. In the concept of sound particle, due to the modelling of the sound source, the spatial distribution of particles follows naturally the same decrease. For example, considering an omnidirectional point source ($Q = 1$), the particle distribution $n(r)$ (in m^2) around the source is equal to:

$$n(r) = \frac{N}{4\pi r^2}. \quad (6)$$

2.2.2.2 Atmospheric absorption Considering the atmospheric absorption, the decrease of the sound intensity after a propagation of distance r , is:

$$I = I_0 \exp -m r = I_0 \exp -\frac{\ln 10}{10} \alpha_{\text{air}} r \quad (7)$$

where I_0 is the initial sound intensity, and m (in Np/m) the atmospheric absorption coefficient, which can be expressed from the atmospheric absorption coefficient α_{air} (in dB/m).

In the SPPS approach, two methods can be considered. With the energetic approach, the particle energy is simply weighted by the amount of decrease along the propagation distance (equation (7)). With the probabilistic method, the atmospheric absorption is considered as the probability that the sound particle disappears or not from the propagation domain, after a propagation distance r :

$$f(r) = \exp -m r. \quad (8)$$

This function is null when r tends to infinity, meaning that the particle cannot propagate to infinity (*i.e.* the particle is absorbed due to air absorption) and is equal to unity for $r = 0$, meaning that the particle cannot be absorbed without propagation. One can also verify that $f(r)$ is a linear function of independent random variables, since:

$$f\left(\sum_{n=1}^N r_n\right) = \prod_{n=1}^N f(r_n). \quad (9)$$

In a practical point of view, the probabilistic method consists in choosing a random number ζ between 0 and 1, at each time step (*i.e.* at each elemental displacement $d_o = c\Delta t$), for each particle, and to compare this number to the probability density function $f(d_o)$. If $\zeta < f(d_o)$ the particle propagates in the domain; if $\zeta \geq f(d_o)$, the particle is absorbed and disappears from the propagation domain.

2.2.2.3 Refraction Considering outdoor sound propagation, sound waves can be refracted due to atmospheric and thermic effects [9]. In the SPPS code, the direction of propagation of a sound particle is then updated at each time step, according to the celerity profile. At the present time, "classical" log-lin profiles are included in the SPPS code [9].

2.2.2.4 Diffusion by fitting objects During propagation, sound particles can be scattered by fitting objects in the propagation domain. If scattering objects are explicitly modeled (*i.e.* objects are included in the 3D-scene), they act following the same procedure than boundary conditions (section 2.2.3). When the number of scattering objects increases in a sub-domain of the propagation domain, the diffusion process that is generated by the multiple scattering, follows a probabilistic approach [10]. Considering a sub-domain of volume V_c , defined by N_c scattering objects (*i.e.*

with a density $n_c = N_c/V_c$) of scattering surface s_c and with an absorption coefficient α_c , then, the probability density function $f(r)$ that a particle collides a scattering object on a distance r is written:

$$f(r) = \nu_c \exp(-\nu_c r), \quad (10)$$

where $\nu_c = 1/\lambda_c$ is the diffusion frequency defined from the mean free path $\lambda_c = 4/(n_c q_c)$.

In practice, the SPPS code uses the method of the cumulative distribution function $p(\hat{R})$ to model the diffusion process, defined by:

$$p(\hat{R}) = \int_0^{\hat{R}} f(R) dR = 1 - \exp(-\nu_c \hat{R}), \quad (11)$$

and giving the probability that a particle encounters a scattering object along a propagation distance \hat{R} . Similarly to the atmospheric absorption, this function is null for $\hat{R} = 0$ and equal to unity for $\hat{R} = \infty$. The numerical simulation of the diffusion process is obtained by considering the inverse cumulative distribution function:

$$\hat{R} = -\frac{1}{\nu_c} \ln [1 - \xi], \quad (12)$$

where ξ is a random number between 0 and 1. Then, for each particle entering into a sub-domain, a random number is considered, giving the distance \hat{R} of collision with a scattering object. When the particle has reached the distance \hat{R} in the sub-domain, the particle is scattered into a new direction according to the reflection law of the scattering object. After collision, a new distance \hat{R} is associated to the particle and the process starts again. The absorption and the reflection processes of a particle by a scattering object follows the same methods than for boundary conditions (see sections 2.2.3.2 and 2.2.3.3).

2.2.3 Boundary conditions

2.2.3.1 Description When a sound wave with unit energy collides with a boundary (wall, object, façades...), a first part R (*i.e.* the reflection coefficient) of the energy is reflected, a second part β is dissipated within the boundary material, and a last part τ (*i.e.* the transmission coefficient) can be transmitted, such as (with α the absorption coefficient):

$$R + \beta + \tau = R + \alpha = 1. \quad (13)$$

2.2.3.2 Absorption and transmission In the probabilistic approach, when sound particles collide with a boundary, the first step is to determine the amount of them that are absorbed or reflected. This is done by comparing a random number u between 0 and 1, for each particle, with the absorption coefficient α . If $u < \alpha$, the particle is absorbed. If this case, a new random number v between 0 and α is chosen. If $v < \tau$, the particle is transmitted, while in the other case, the particle simply disappears from the propagation medium. Lastly, if $u \geq \alpha$, the particle is reflected according to the reflection law of the boundary (section 2.2.3.3).

In the energetic approach, the energy of the particle is weighted by the reflection coefficient R . Then, the particle is reflected according to the reflection law of the boundary. Here again, a part β of the energy of the particle can be dissipated within the material, while another part τ can be transmitted. If transmission occurs, a new particle is created with an initial energy τ .

2.2.3.3 Reflection In room acoustics, it is usual to consider that reflection can be split into a specular part and a diffuse part, the ratio being defined by the scattering coefficient s [2]. For both approaches, a random number w is chosen between 0 and 1. If $w < 1 - s$ the particle is reflected specularly, while, in the other case, the reflection is chosen according to the diffuse reflection law. One can remark that the duplication of the particle (one in the specular direction, and the duplicate one in the diffusion reflection) is not implemented in the SPSS code yet. Another solution could also consist in considering a single reflection law instead of splitting into two reflections.

Let us consider now an incident particle on a boundary, with an incident direction defined by spherical coordinates (θ, ϕ) . We can define the probability $P(\theta, \phi; \theta', \phi') \equiv P(\Omega, \Omega')$ that the particle is reflected in the solid angle $d\Omega' = \sin \phi' d\phi' d\theta'$. Lastly, we can also consider the incident flux of particles $j(\theta, \phi)$ on the boundary. Finally, the reflected flux $j'(\theta', \phi')$ must be verified:

$$j'(\theta', \phi') \cos \phi' = \int P(\theta, \phi; \theta', \phi') j(\theta, \phi) \cos \phi d\Omega, \quad (14)$$

which can also be written:

$$j'(\theta', \phi') = \int R(\theta, \phi; \theta', \phi') j(\theta, \phi) \cos \phi d\Omega. \quad (15)$$

where $R(\theta, \phi; \theta', \phi')$ is the reflection law.

Several reflection laws have been implemented in the SPSS code, from which, one can cite for example, the specular one:

$$R(\theta, \phi; \theta', \phi') = 2\delta(\theta - \theta' \pm \pi) \delta(\sin^2 \phi - \sin^2 \phi'), \quad (16)$$

with δ the Dirac distribution, the Lambert's one:

$$R(\theta, \phi; \theta', \phi') = \frac{1}{2\pi} \times 2, \quad (17)$$

and the uniform one:

$$R(\theta', \phi') = \frac{1}{2\pi \cos \phi'}, \quad (18)$$

with $\theta' \in [0, 2\pi]$ and $\phi' \in [0, \pi/2]$.

In practice, the direction of reflection is obtained with the method of the inverse cumulative distribution function (see section 2.2.2.4). It can be noted that for the uniform and Lambert reflections, reflection laws are only function of ϕ' , the angle θ' being uniform between 0 and 2π . When the last method can not be applied (*i.e.* for complex reflection laws), the rejection method can also be used.

2.2.4 Sound field calculation

2.2.4.1 Volume receiver Since punctual receivers cannot be numerically defined, they must be modeled as a spherical volume with a volume V_{rec} . Then, the total energy $E_{\text{rec}}^j(n)$ for a given receiver, at time step n , in the frequency band j , is the sum of the energy ϵ_i^j of each particle passing through the receiver, at the same time step:

$$E_{\text{rec}}^j(n) = \sum_i^{N_0} \epsilon_i^j = \sum_i^{N_0} \frac{W}{N} \epsilon_i^j \times \Delta t_i, \quad (19)$$

where N_0 is the total number of particles passing through the receiver volume, $\Delta t_i = \ell_i/c$ is the path duration of the

particle in the receiver volume (ℓ_i is the path length and c the speed of sound), and ϵ_i^j the energy weighting coefficient for the particle i . In the probabilistic approach, ϵ_i^j is equal to unity. In the energetic approach, ϵ_i^j expresses the amount of energy that is dissipated during the last time step by the particle i , due to all physical phenomena occurring during the past propagation. Finally, the energy density $w_{\text{rec}}^j(n)$ (in J/m^3) at a receiver is given by:

$$w_{\text{rec}}^j(n) = \frac{E_{\text{rec}}^j(n)}{V_{\text{rec}}} = \frac{W}{N} \frac{1}{V_{\text{rec}}} \sum_i^{N_0} \epsilon_i^j \frac{\ell_i}{c}. \quad (20)$$

In addition, the intensity $I_{\text{rec}}^j(n)$ and the intensity vector $\mathbf{I}_{\text{rec}}^j(n)$ (in W/m^2) are given by:

$$I_{\text{rec}}^j(n) = c \times w_{\text{rec}}^j(n) = \frac{W}{N} \frac{1}{V_{\text{rec}}} \sum_i^{N_0} \epsilon_i^j \ell_i, \quad (21)$$

with c the speed of sound, and

$$\mathbf{I}_{\text{rec}}^j(n) = \frac{W}{N} \frac{1}{V_{\text{rec}}} \sum_i^{N_0} \epsilon_i^j \ell_i \frac{\mathbf{v}_i}{c_i}, \quad (22)$$

where \mathbf{v}_i is the velocity of the particle i , of norm c_i . It must be noted that the norm of $\mathbf{I}_{\text{rec}}^j(n)$ is not equal to $I_{\text{rec}}^j(n)$.

2.2.4.2 Surface receiver The sound power W_{surf}^j (in W) received by a elemental surface of size ΔS with normal \mathbf{n} , in the frequency band j , is the sum of the energy carried by each particle i , by unit of time Δt , at time step n :

$$W_{\text{surf}}^j(n) = \sum_i^{N_0} \frac{\epsilon_i^j}{\Delta t} \frac{\mathbf{v}_i}{c} \cdot \mathbf{n} = \frac{W}{N} \sum_i^{N_0} \epsilon_i^j \cos \theta_i, \quad (23)$$

where θ_i is the angle between the normal \mathbf{n} and the particle velocity \mathbf{v}_i , and N_0 the total number of particles that collide the surface. The sound intensity $I_{\text{surf}}^j(n)$ (in W/m^2) received by the elemental surface ΔS at the time step n is then:

$$I_{\text{surf}}^j(n) = \frac{W}{N} \frac{1}{\Delta S} \sum_i^{N_0} \epsilon_i^j \cos \theta_i. \quad (24)$$

2.3 SPSS code

The SPSS code is an implementation of the energetic and the probabilistic approaches. Although SPSS can run as a stand alone executable program, its use can be greatly simplified by the use of the I-Simpa graphical user interface (I-Simpa.ifsttar.fr) [11]. I-Simpa allows to run the SPSS code for complex geometries and to post-process the numerical results. In particular, room acoustics parameters can be calculated and several graphical representations can be displayed.

A specific documentation is propose to explain the implementation of the method in the SPSS code, with a specific attention to the optimization and the validation of the algorithms. As it seems not pertinent here to give more details on this implementation, readers can consult the SPSS documentation [12] given with I-Simpa.

3 Validations

This section presents some validations of the SPSS code for several room acoustics applications. More validations are given in the SPSS documentation [12].

Table 1: EDT (in s) comparison between the SPPS code and the radiosity method [3, from figure 2.21, page 57].

Rec.	1	2	3	4	5	6	7	8	9
Line 1									
Kang	1.05	0.90	—	0.99	1.24	1.30	1.32	1.30	1.30
SPPS	1.15	1.08	—	1.19	1.25	1.28	1.28	1.29	1.29
Line 2									
Kang	1.26	1.26	1.26	1.23	1.24	1.27	1.29	1.27	1.27
SPPS	1.27	1.26	1.24	1.24	1.25	1.25	1.27	1.27	1.28
Line 3									
Kang	1.30	1.30	1.30	1.27	1.24	1.24	1.25	1.25	1.27
SPPS	1.27	1.26	1.25	1.25	1.25	1.26	1.28	1.28	1.27

Table 2: Absorption and scattering coefficients configurations of the flat room.

Configuration #1						
Wall	Floor	Ceiling	Left	Right	Ext. 1	Ext. 2
α	0.9	0.1	0.3	0.3	0.6	0.6
s	0 : 0.2 : 1					
Configuration #2						
α	1.0	0	0	0	0	0
s	1 (Lambert's reflection)					

3.1 Cubic rooms

Here, we compare the SPPS results with the radiosity method (*i.e.* the scattering coefficient is equal to 1) for a cubic room of size $10 \times 10 \times 10 \text{ m}^3$ with uniform absorption $\alpha = 0.2$. The sound source is located at (3, 3, 3) m. Results are given in terms of early decay times (EDT) for three receivers lines (9 receivers per line) along the diagonal lines [3].

SPPS simulations have been performed with 1 million of particles, a time step of 2 ms and a duration of 2 s, without atmospheric absorption, using the energetic approach. Table 1 shows that the agreement between both approaches is very good, with mean deviations less than 0.07 s. As expected for a cubic room with low and uniform absorption, EDT values are almost uniform for all receivers, except closed to the source (receivers 1-4 on line 1), and are very closed to the value 1.33 s obtained with the Sabine's formula.

3.2 Flat rooms

In this section, we compare the SPPS code with numerical simulations realized by Korany *et al.* [13] with a hybrid ray-tracing and image-sources based method, taking diffusely reflecting boundaries into account. A rectangular long flat room of size $20 \times 30 \times 10 \text{ m}^3$ is considered with a sound source ($L_W = 0 \text{ dB}$) at (2.5, 15, 3) m. Results are given at a receiver at (15, 10, 4) m for several values of the scattering coefficient s and absorption coefficient α (table 2).

SPPS simulations have been performed with 1 million of particles, a time step of 2 ms and a duration of 1.5 s, using the probabilistic approach. Comparisons are given in terms of reverberation times (RT30) for both configurations at table 3. Although it is not really applicable for long room with a non-uniform absorption distribution, results are also compared with the classical Sabine and Eyring's formula. Results show a very good agreement between both numerical methods, with differences less than 10%, and decreasing with s . One can remark that the SPPS code gives very good results for

Table 3: RT30 comparisons between SPPS and Korany numerical simulations, and with the Sabine and Eyring formula, for configurations #1 and #2 of table 2.

	#1						#2
s	0.0	0.2	0.4	0.6	0.8	1.0	1.0
Korany	1.13	0.98	0.76	0.68	0.69	0.72	1.09
SPPS	1.29	0.87	0.80	0.74	0.72	0.69	1.11
Sabine	0.96						1.63
Eyring	0.71						1.40

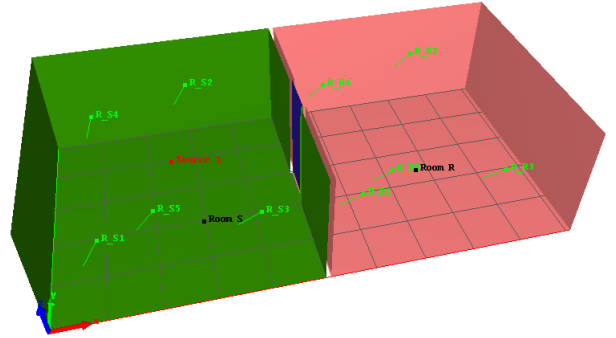


Figure 1: Coupled rooms geometry. See table 4 for details.

specular reflections ($s = 0$), while the approaches (particle-tracing for SPPS and image-sources for Korany) are very different.

3.3 Coupled rooms

Here, we consider two rooms S (with the source) and R (without the source) of same size $5 \times 5 \times 2.5 \text{ m}^3$, coupled through a door of size $0.9 \times 2.5 \text{ m}^2$ (figure 1). Walls are perfectly diffuse and defined by a uniform absorption coefficient (without transmission). The sound source ($L_W = 100 \text{ dB}$) is located on the center of the first room S at position (2.5, 2.5, 1.25) m. Sound levels are calculated for 5 receivers on each room, and then, averaged per room in order to estimate the sound level difference $\Delta = L_S - L_R$ between rooms.

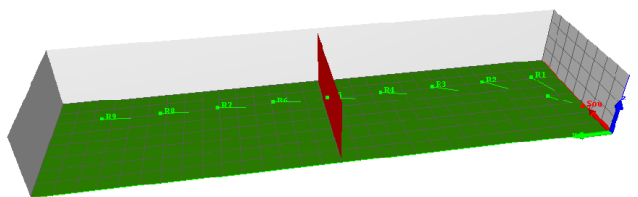
Numerical results have been obtained with 1 million of particles, a time step of 10 ms and a duration of 1.5 s, using the probabilistic approach. Atmospheric absorption has not been considered. Calculations have been carried out for several values of the absorption coefficient of the rooms, as well as for several values of the transmission loss R (in dB) and absorption coefficient of the door. Results are shown at table 4 and are compared to the classical theory of coupled rooms, with a very good agreement.

3.4 Fitted rooms (industrial halls)

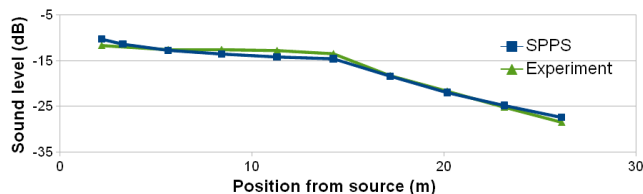
In this section, we compare the SPPS code with experimental data obtained in a testing room of size $30 \times 8 \times 3.85 \text{ m}$ [14]. Walls are specularly reflecting, with an absorption coefficient of 0.1 for lateral walls, 0.05 for the floor and 0.15 for the ceiling. The fitting zone is localized in the second part of the room (with a regular repartition on the surface) and is made with 80 objects of size $0.5 \times 0.5 \times 3 \text{ m}^3$, and absorption $\alpha_c = 0.3$ (figure 2(a)). The sound source is located at position (1.5, 1, 0.85) m. Sound level measurements have been realized along a receiver

Table 4: Sound level difference $\Delta = L_S - L_R$ between two coupled rooms (figure 1). Comparison between numerical results (SPPS) and the classical theory of coupled rooms.

Absorption coefficient			R (dB) Door	SPPS	Theory
Room S	Room R	Door			
0.1	0.1	1.0	0	7.58	7.29
0.1	0.3	1.0	0	11.81	11.49
0.3	0.3	1.0	0	11.65	11.49
0.3	0.1	1.0	0	7.28	7.29
0.05	0.5	1.0	0	14.09	13.58
0.5	0.05	1.0	0	4.59	5.02
0.1	0.3	0.1	20	31.32	31.20
0.1	0.3	0.1	10	21.20	21.20
0.1	0.3	0.2	10	21.28	21.23



(a) Geometry of the fitting zone and receivers locations



(b) Sound level comparison (2 kHz octave band)

Figure 2: Comparison between experimental sound levels in a fitting room with SPPS numerical results.

line (4.0, 3 : 3 : 27, 1.5) m for the 2 kHz octave band, and normalized by the reference microphone at (2, 3, 1.5).

Numerical simulations have been carried out with 1 million of sound particles, a time step of 5 ms and a duration of 1.5 s, using the energetic approach. As shown at figure 2(b), a very good agreement is obtained with a maximum sound level difference of 1.4 dB. Complementary simulations for the same room but with other fitting configurations (empty room, fitting in the entire room, fitting in the first part of the room only) show also a very good agreement [12].

4 Conclusion

The particle-tracing method is a very efficient method for the sound field modelling in architectural acoustics. Although, this papers focusses only on room acoustics applications, the method can also be applied to outdoor sound propagation. In comparison with ray-tracing or source-images based methods (or similar), the particle method allows to consider "events" along the propagation, such as diffusion by fitting objects or changes of propagation direction (refraction), which can be of interest in several applications.

The method has been implemented in the SPPS code with a special attention to the reduction of the computation times.

As the SPPS code has been included in the I-Simpa software (`i-simpa.ifsttar.fr`), it can be used as an operational tool for researchers and engineers. However, it must be noted that the diffraction phenomena is not implemented yet.

References

- [1] M. Vorländer, *Auralization: fundamentals of acoustics, modelling, simulation, algorithms and acoustic virtual reality*, Springer-Verlag, Berlin (2008)
- [2] H. Kuttruff, *Room acoustics*, Spon Press, London (2000)
- [3] J. Kang, *Acoustics of long spaces: theory and design practice*, Thomas Telford Publishing, London (2002)
- [4] K. Kowalczyk, M. van Walstijn, "Room Acoustics Simulation Using 3-D Compact Explicit FDTD Schemes", *Audio, Speech, and Language Processing, IEEE Transactions on* **19**(1), 34-46 (2011)
- [5] Y. Kagawa, T. Tsuchiya, K. Fujioka, M. Takeuchi, "Discrete Huygens' model approach to sound wave propagation-reverberation in a room, sound source identification and tomography in time reversal", *Journal of Sound and Vibration* **225**, 61-78 (1999)
- [6] W.B. Joyce, "Sabine's reverberation time and ergodic auditorium", *Journal of the Acoustical Society of America* **58**(3), 643-655 (1975)
- [7] U. Stephenson, "Comparison of the mirror image source method and the sound particle simulation method", *Applied Acoustics* **29**, 35-72 (1990)
- [8] J. Picaut, "Numerical application of the concept of sound particles to modeling sound fields in architectural acoustics", *Bulletin des laboratoires des Ponts et Chaussées* **258-259**, 59-88 (2005)
- [9] E.M. Salomons, *Computational atmospheric acoustics*, Kluwer Academic Publishers, Dordrecht (2001)
- [10] H. Kuttruff, "Sound decay in reverberation chambers with diffusing elements", *Journal of the Acoustical Society of America* **69**(6), 1716-1723 (1981)
- [11] J. Picaut, N. Fortin, "I-Simpa, a graphical user interface devoted to host 3D sound propagation numerical codes", *Acoustics 2012 Nantes Conference* (2012)
- [12] J. Picaut, N. Fortin, *Manuel de référence du code SPPS* (in French), Ifsttar (2011)
- [13] N. Korany, J. Blauert, O. Abdel Alim, "Acoustic simulation of rooms with boundaries of partially specular reflectivity", *Applied Acoustics* **62**, 875-887 (2001)
- [14] A.M. Ondet, J.L. Barbry, "Modeling of sound propagation in fitted workshops using ray tracing", *Journal of the Acoustical Society of America* **85**(2), 787-796 (1989)